HHS Public Access

Author manuscript

Proc SPIE Int Soc Opt Eng. Author manuscript; available in PMC 2016 February 09.

Published in final edited form as:

Proc SPIE Int Soc Opt Eng. 2015 March 17; 9417: . doi:10.1117/12.2082173.

Micro-Computed tomography (CT) based assessment of dental regenerative therapy in the canine mandible model

P. Khobragade[1,2], **A. Jain**[2], **S. V. Setlur Nagesh**[2], **S. Andreana**[3], **R. Dziak**[4], **S. K. Sunkara**[4], **S. Sunkara**[4], **D. R. Bednarek**[2], **S. Rudin**[1,2], and **C. N. Ionita**[1,2]

[1]Department of Biomedical Engineering, State University of New York at Buffalo

[2]Toshiba Stroke and Vascular Research Center, State University of New York at Buffalo

[3]Department of Restorative Dentistry, State University of New York at Buffalo

[4]Department of Oral Biology, State University of New York at Buffalo

Abstract

High-resolution 3D bone-tissue structure measurements may provide information critical to the understanding of the bone regeneration processes and to the bone strength assessment. Tissue engineering studies rely on such nondestructive measurements to monitor bone graft regeneration area. In this study, we measured bone yield, fractal dimension and trabecular thickness through micro-CT slices for different grafts and controls. Eight canines underwent surgery to remove a bone volume (defect) in the canine's jaw at a total of 44 different locations. We kept 11 defects empty for control and filled the remaining ones with three regenerative materials; NanoGen (NG), a FDA-approved material (n=11), a novel NanoCalcium Sulfate (NCS) material (n=11) and NCS alginate (NCS+alg) material (n=11). After a minimum of four and eight weeks, the canines were sacrificed and the jaw samples were extracted. We used a custom-built micro-CT system to acquire the data volume and developed software to measure the bone yield, fractal dimension and trabecular thickness. The software used a segmentation algorithm based on histograms derived from volumes of interest indicated by the operator. Using bone yield and fractal dimension as indices we are able to differentiate between the control and regenerative material ($p<0.005$). Regenerative material NCS showed an average 63.15% bone yield improvement over the control sample, NCS+alg showed 55.55% and NanoGen showed 37.5%. The bone regeneration process and quality of bone were dependent upon the position of defect and time period of healing. This study presents one of the first quantitative comparisons using non-destructive Micro-CT analysis for bone regenerative material in a large animal with a critical defect model. Our results indicate that Micro-CT measurement could be used to monitor in-vivo bone regeneration studies for greater regenerative process understanding.

2. Introduction

The work presented here is an analysis to correlate the imaging based quantitative analysis with the pathology of dental regenerative material in a canine mandible using Micro-CT. Nearly one million individuals suffer from fracture due to bone disease in the United States alone. Regenerative material based healing therapies with added nanotechnology based material are among the current trends in healing bone injuries [1, 2].

Different products for bone regeneration are getting commercialized. Each material presents particular features of the regeneration mechanism which leads to different healing results. Advanced micro-imaging methods have a large impact for evaluation and understanding of the graft based bone regeneration. Micro-CT imaging is the golden standard technique for evaluation of bone microstructure in ex vivo [3] and in vivo studies [4, 5] in small animal models [6, 7].

Bone is majorly classified into trabecular and cortical structures [8]. Bone mineral density is the most important factor for bone strength determination [9, 10]. Several studies reported that, along with trabecular bone structure, structural change in cortical bone is an indicator of bone mineral density (BMD). Trabecular and cortical bone are useful in assessing the bone strength and differentiating between healthy individuals and patients with osteoporotic fractures [11, 12]. Quantitative and qualitative analyses of bone regeneration can be done through imaging based parameters extracted from trabecular and cortical bone structures.

There are many studies done on small animal models for evaluation of regenerative material [13–15]. However, there appears to be a scarcity of comparisons of different regenerative materials on large animal models such as canines with large defect models which closely mimic bone defects in humans. Bone regeneration is animal model dependent [16], hence the material should be evaluated with different large animal models before human treatment. Factors such as healing time period and mechanical factors due to defect position may play a key role in bone regeneration which should be evaluated.

Imaging based parameters such as bone volume [17], bone volume fraction [18], fractal dimension [19] and trabecular thickness [18] are usually used to analyze bone regeneration and correlate structure with pathology. Such parameters are common with other imaging modalities such as MRI and Ultrasound [20, 21], and have been investigated to understand how they relate with bone regeneration process.

In this proceeding we compare regenerative outcomes for three materials (NanoGen (NG), NanoCalcium Sulfate (NCS) and NCS alginate (NCS+alg), using four imaging based parameters: bone yield, trabecular thickness and fractal dimension. We considered the time and the defect position as factors responsible for generating these responses. We found that the three materials' bone regeneration is significantly superior to that of the control samples (untreated). The time period and defect position are significant factors for comparing the outcomes of materials. These results indicate the application of micro-CT based imaging parameters are useful for quantifying the outcomes of regenerative material and also these parameters can be helpful for quantifying biological activities.

3. Materials and Methods

We carried out this study in three parts. In the first part we present sample preparation details and surgery procedure. In the second part, we describe the system, data acquisition procedure and reconstruction. In the third part, we describe the LabVIEW based program development for the imaging based parameters calculation and the statistical and sensitivity analysis.

3.1 Sample preparation

Eight canines underwent surgery. We removed a bone volume (defect) at three places in the mandible of each canine, in all we removed the bone volume in (n= 44) sites as shown in Figure (1). In these sites a small base of the bone was left to support the material. Critical size defects in the range of 335 mm^3 to 684 mm^3 were created so these wounds will not have healed throughout the lifetime of the animal [22]. We filled the defects with three regenerative materials: NanoGen (n= 11), NanoCalcium Sulfate (n=11), and NanoCalcium Sulfate alginate (n=11). We kept (n= 11) samples empty for control. After filling the material in the defect position we closed the defect by sutures. For identification purposes we drilled the defect boundaries and inserted titanium screws between each defect. These screws served as an identification marker while analyzing the radiographic images.

NanoGen is an FDA approved material made of small calcium sulfate grains which was recently launched by Orthogen LLC. Nano Calcium Sulfate (NCS) is a material composed of nano-sized calcium sulfate crystals fabricated by our lab and protected by U.S patent 7767226 issued on October 2010 [23]. Nano Calcium Sulfate alginate (NCS+alg) is a mixture of Nano Calcium Sulfate and 10% alginate, a natural polysaccharide. Alginate has been shown to enhance the delivery of mesenchymal stem cells as well as growth factors such as bone morphogenetic protein relative to the nanoproduct without the alginate [24].

The canines were sacrificed after four and eight week time periods. The jaw samples were extracted and stored in formalin solution. We used two different time intervals in order to test the effect of the time interval on the bone regeneration. The specific time periods were chosen in such way that there should not be significant natural growth taking place in the control samples and we could confidently compare the outcomes of regenerative material. The experiment design gave us an opportunity to validate and quantify different biological parameters such as time and defect position on bone regeneration.

3.2 Data acquisition

We used a custom built micro-CT system [25] as shown in Figure (2). The system consists of a high resolution micro angiographic fluoroscope (MAF) detector [26] developed in our lab and a micro-focus Ultrabright Oxford x-ray tube with XYZ rotary stage for the sample mounting purpose. The detector has a 1024×1024 matrix with an effective pixel size of 43 microns [27]. We scanned the entire samples with a tube voltage of 60 kVp and tube current of 1 mA, SID and SOD of 82 cm and 78 cm, respectively. We kept all technique parameters constant for every sample. The canine mandibles were dried using gauze before being mounted on the rotary stage on the Micro-CT. To avoid the relative change in the position of an object as the stage rotates we fixed the samples on the holder using fixing tape.

Projection images were acquired and then reconstructed using the FDK algorithm [28]. All the imaging techniques followed guidelines given by Bouxsein et al in the Journal of Bone and Mineral Research [29] such as constant scanning parameters, aluminum filter placement for beam hardening correction, proper sample preparation and positioning. For proper interpretation of 3D slice data we defined the co-ordinate system which is shown in figure

(3). The sagittal view showed the best orientation of the scan with regard to the canine anatomy. All our results are reported with regard to the convention depicted in Figure (3).

3.3 Data analysis

We developed LabVIEW GUI software for calculation of imaging based parameters such as bone yield, trabecular thickness and fractal dimension. This program was based on a specimen specific threshold technique which provides the option for choosing a maximum and minimum value of the threshold. In the literature there is no consensus on thresholding technique [29]; we chose a specimen specific threshold because samples were taken from two different time intervals. After thresholding, we drew the ROI contour. We counted the total number of volume elements falling inside the chosen volume of interest (VOI) throughout the data volume and multiplied by the volume element size to get the actual physical volume of regenerated bone. The volume of bone removed at each place in the canine mandible was not constant because of asymmetric biological structure as shown in Figure (4).

In order to compare outcomes of all materials in one platform we decided to calculate the bone yield. Bone yield is a ratio of volume of bone in a given region of interest (ROI) to total volume of the ROI. Bone yield quantifies the bone regenerated per unit volume.

$$Bone\ yield\ (BY) = \frac{Volume\ of\ regenerated\ Bone}{Total\ volume\ of\ interest}$$

We calibrated our system using a cylindrical object with known volume and a density close to that of bone. We obtained 98% accuracy in calculating the volume through the program. Fractal analysis is a quantitative tool to study the morphology of the intricate structure and has been shown to have application in dentistry [19]. Researchers had found a strong correlation between the fractal dimension and bone mineral density [30, 31]. In our experiment, we measured the complexity of natural bone growth with respect to artificially regenerated bone growth. In order to calculate the fractal dimension we first separate the ROI volume by cropping the reconstructed images. On each ROI volume we calculated fractal dimension by a box counting algorithm [32].

3.3.1 Statistical analysis—To quantify differences in our sample population considering three responses and three factors, we designed the statistical experiment model to analyze the effect of each factor on each response, as shown in Figure (5). The boxes on the left side represents three factors responsible for generating three responses in the boxes on the right side. We performed an analysis of variance (ANOVA) to find which factors were significant in the generating three responses. Statistical analysis was performed using Minitab software. Significance level was set at $p<0.05$. We used a general linear model to statistically test the difference between control and regenerative material by considering three factors such as material type, time period and sample position

3.3.2 Sensitivity analysis—Calculating quantitative imaging parameters from threshold images adds uncertainty in reproducibility of data. Manual thresholding techniques are dependent on the data operator and there is not any single segmentation technique that can be able to segment all kind of images. We used specimen specific thresholding as densities of bone varies on different canine samples and defect position. In order to test the reproducibility of the experiment, we presented the sensitivity analysis. We compared 2D slice by slice difference between the original and segmented sample to ensure the accuracy of segmentation. To test the effect of the segmentation uncertainty, we checked the sensitivity of parameter, bone volume (BV) and bone yield (BY) by changing the threshold values by ±2% of our chosen threshold values.

4. Result

A new LabVIEW graphic user interface software has been developed. Direct visualization of reconstructed samples is shown in Figure (6). The area of defect is between the two metal screws and is indicated with a dashed square. The top row displays a control sample as it can be seen in the outlined area; there is some bone regeneration due to the natural healing processing. The NanoGen sample in the second row showed better defect filling than the control. Finally NCS and NCS+alg showed the best results. By manual visualization through the slice, differences were clearly visible as shown in Figure (6). Visual perceptible difference was observed in temporal comparison of the samples.

Bone growth in control samples with respect to the eight week and four week time period is shown in figure 7(a). The top row shows three different views from the four week sample and bottom row shows three different views from an eight week sample. Similar comparisons were done with samples treated using regenerative material: figure 7(b) with NanoGen, figure 7(d) with NCS and figure 7(c) with NCS+alginate. In order to quantify the visible differences, we calculated different imaging based parameters such as bone yield, fractal dimension and trabecular thickness. There was a significant difference in bone yield due to the three different regenerative materials and control samples. The average bone yield values for eight and four week samples were: 13 ± 0.05 for the control, 19 ± 0.03 for NanoGen, 25 ± 0.05 for NCS and 23 ± 0.04 for NCS+alg as seen in Figure 8(d). The average three dimensional fractal for eight and four week samples were: 2.20 ± 0.08 for the control, 2.29 ± 0.05 for NanoGen, 2.32 ± 0.09 for NCS and 2.22 ± 0.09 for NCS+alg as seen in Figure 8(a).

The average trabecular thicknesses measure in pixels for eight and four week samples were: 27 ± 9 for the control, 28 ± 7 for NanoGen, 30 ± 9 for NCS and 28 ± 8 for NCS+alg as shown in Figure 8(b). Regenerative material NCS showed an average 63.15% bone yield improvement over the control sample, 55.55% using NCS+alg and 37.5% using NanoGen as seen in Figure 8(c). Quantitative values for eight and four week samples were shown in table 1. Quantitative values were different if compared according to two different time intervals and three different positions within a single canine mandible.

We found that the material type and implant positions were significant factors while considering “bone yield” as a response ($p<0.0001$). Material type and time were significant

factors while considering “fractal dimension” as a response ($p<0.0001$). Implant position was significant while considering “trabecular thickness” as a response ($p<0.001$). Material type and time were not significant factors while considering “trabecular thickness” as a response.

The sensitivity analysis, by changing the threshold values by ± 2% with respect to our chosen threshold values revealed that bone volume and bone yield changed on average by 19% and 22%. The sample-wise sensitivity is shown in Figure 9 (a, b, c, d). STD_thresh is the threshold value chosen by us, ‘+’2% and ‘−’2% STD is ± 2% percentage with respect to our chosen threshold value. The average change in bone volume and bone yield by changing the threshold values by ± 2% is shown in Figure 9 (e). The average manual error that might be caused in choosing the threshold values were significantly lower than the difference in the quantitative values we calculated for each element. Hence the errors due to the operator are less likely to lead to faulty conclusions regarding the benefit of one material over another.

5. Discussion

In this study, we have assessed the correlation of imaging based parameters with pathology of dental regenerative therapy for in vivo characterization of trabecular structure due to different regenerative materials. An image processing technique with box counting algorithm has been implemented in order to accesses the outcomes of dental regenerative material from high resolution micro-CT acquisition. Regenerative material NCS showed an average of 63.15% bone yield improvement over the control sample, NCS+alg 55.55% and NanoGen 37.5%. Imaging based parameter bone yield was found to be significantly different between regenerative materials and control ($p<0.001$). There was a slight difference between the three regenerative materials but still the difference is such that we can quantitatively compare the outcomes. We found that the position of the defect (position from where volume of bone is removed) effect was significantly different if compared in each mandible for the same material. This difference might be due to mastication stress differences. Time was not a significant factor for bone yield comparison since it might be that after the first few weeks, trabecular structure starts changing to cortical structure without actually increasing the volume of bone regenerated.

Fractal dimension is descriptive of bone mineral density (BMD) and is shown to be significantly different between regenerative material ($p<0.001$). It was also significantly different if compared with relation to time ($p<0.001$). The difference in fractal dimension with respect to time showed that the BMD was continuing to increase until the eighth week of the time period. Fractal dimension interpreted as the complexity of the object and by statistical analysis revealed that the eight week samples grew out to be more complex as compared to the four week samples. We did not find any significant difference in trabecular thickness for control and regenerated samples which shows that the bone regeneration due to the artificial implanted material has similar trabecular structure as that of natural bone.

In this study we did the sensitivity analysis by varying the segmentation limit by ±2%. As there is no consensus for choosing standard threshold values, sensitivity analysis may

provide information about the reproducibility of parameter calculation. We found that the error that might be introduced due to the segmentation was significantly less than our calculated quantitative values. Segmentation is the most sensitive part of a calculation and by testing the segmentation sensitivity we can ensure the reproducibility of data.

The microangiographic fluoroscope (MAF) detector used in this experiment is a similar detector to that which is mounted on a clinical angiographic suite. This experiment showed the possible application of the MAF detector for in vivo time lapse Micro –computed tomography for large animal models. In vivo time lapse studies could possibly reduce the cost of experiments spent on a large population of animal models.

6. Conclusion

By using imaging based parameters derived from high resolution micro-CT, we were able to differentiate between regenerative material and control samples. NCS and NCS+alg showed more or similar growth as compared to the FDA approved material NanoGen. All the regenerative material showed significantly more growth as compared with the control samples. The bone regeneration process and bone quality were dependent upon the defect position and time period. Sensitivity analysis showed that quantitative imaging data are reproducible. The radiographic micro-angiographic fluoroscopic detector used in this experiment is the same that is used in clinical-research C-arm or angiographic systems. This kind of experiment can be extrapolated to clinical settings for C-arm cone beam computed tomography. This is the first kind of study with a large animal model with critical size defects treated with novel regenerative nanomaterial. We evaluated the data obtained with different metrics such as bone yield, fractal dimension and trabecular thickness. This kind of quantitative data can be used in standardizing systems and used as a reference for further upcoming studies.

Acknowledgments

This work is supported in part by NIH Grant: 2R01EB002873, The Bruce Holm Memorial Catalyst Fund (UB STOR) and an equipment grant from Toshiba Medical Systems Corporation

References

1. Kallai I, Mizrahi O, Tawackoli W, Gazit Z, Pelled G, Gazit D. Microcomputed tomography-based structural analysis of various bone tissue regeneration models. Nat Protoc. Jan.2011 6:105–10.
2. Sittinger M, Hutmacher DW, Risbud MV. Current strategies for cell delivery in cartilage and bone regeneration. Curr Opin Biotechnol. Oct.2004 15:411–8.
3. Laib A, Barou O, Vico L, Lafage-Proust MH, Alexandre C, Rugsegger P. 3D micro-computed tomography of trabecular and cortical bone architecture with application to a rat model of immobilisation osteoporosis. Med Biol Eng Comput. May.2000 38:326–32.
4. Boyd SK, Davison P, Muller R, Gasser JA. Monitoring individual morphological changes over time in ovariectomized rats by in vivo micro-computed tomography. Bone. Oct.2006 39:854–62.
5. Waarsing JH, Day JS, van der Linden JC, Ederveen AG, Spanjers C, De Clerck N, et al. Detecting and tracking local changes in the tibiae of individual rats: a novel method to analyse longitudinal in vivo micro-CT data. Bone. Jan.2004 34:163–9.
6. Schambach SJ, Bag S, Schilling L, Groden C, Brockmann MA. Application of micro-CT in small animal imaging. Methods. Jan.2010 50:2–13.

7. Genant HK, Engelke K, Prevrhal S. Advanced CT bone imaging in osteoporosis. Rheumatology (Oxford). Jul; 2008 47(Suppl 4):iv9–16.
8. Seeman E, Delmas PD. Bone quality--the material and structural basis of bone strength and fragility. N Engl J Med. May 25.2006 354:2250–61.
9. Ulrich D, van Rietbergen B, Laib A, Ruegsegger P. The ability of three-dimensional structural indices to reflect mechanical aspects of trabecular bone. Bone. Jul.1999 25:55–60.
10. Muller R, Van Campenhout H, Van Damme B, Van Der Perre G, Dequeker J, Hildebrand T, et al. Morphometric analysis of human bone biopsies: a quantitative structural comparison of histological sections and micro-computed tomography. Bone. Jul.1998 23:59–66.
11. Seeman E, Delmas PD, Hanley DA, Sellmeyer D, Cheung AM, Shane E, et al. Microarchitectural deterioration of cortical and trabecular bone: differing effects of denosumab and alendronate. J Bone Miner Res. Aug.2010 25:1886–94.
12. Wachter NJ, Krischak GD, Mentzel M, Sarkar MR, Ebinger T, Kinzl L, et al. Correlation of bone mineral density with strength and microstructural parameters of cortical bone in vitro. Bone. Jul. 2002 31:90–5.
13. Plachokova AS, van den Dolder J, Stoelinga PJ, Jansen JA. The bone regenerative effect of platelet-rich plasma in combination with an osteoconductive material in rat cranial defects. Clin Oral Implants Res. Jun.2006 17:305–11.
14. Gauthier O, Muller R, von Stechow D, Lamy B, Weiss P, Bouler JM, et al. In vivo bone regeneration with injectable calcium phosphate biomaterial: a three-dimensional micro-computed tomographic, biomechanical and SEM study. Biomaterials. Sep.2005 26:5444–53.
15. Requicha JF, Moura T, Leonor IB, Martins T, Munoz F, Reis RL, et al. Evaluation of a starch-based double layer scaffold for bone regeneration in a rat model. J Orthop Res. Jul.2014 32:904–9.
16. Pearce AI, Richards RG, Milz S, Schneider E, Pearce SG. Animal models for implant biomaterial research in bone: a review. Eur Cell Mater. 2007; 13:1–10.
17. Swain MV, Xue J. State of the art of Micro-CT applications in dental research. Int J Oral Sci. Dec. 2009 1:177–88.
18. Kontogiorgos E, Elsalanty ME, Zapata U, Zakhary I, Nagy WW, Dechow PC, et al. Three-dimensional evaluation of mandibular bone regenerated by bone transport distraction osteogenesis. Calcif Tissue Int. Jul.2011 89:43–52.
19. Sánchez UG II. Fractals in dentistry. Journal of dentistry. 2011; 39:273–292.
20. Luo G, Kaufman JJ, Chiabrera A, Bianco B, Kinney JH, Haupt D, et al. Computational methods for ultrasonic bone assessment. Ultrasound Med Biol. Jun.1999 25:823–30.
21. Eckstein F, Burstein D, Link TM. Quantitative MRI of cartilage and bone: degenerative changes in osteoarthritis. NMR Biomed. Nov.2006 19:822–54.
22. Huh JY, Choi BH, Kim BY, Lee SH, Zhu SJ, Jung JH. Critical size defect in the canine mandible. Oral Surg Oral Med Oral Pathol Oral Radiol Endod. Sep.2005 100:296–301.
23. Park YB, Mohan K, Al-Sanousi A, Almaghrabi B, Genco RJ, Swihart MT, et al. Synthesis and characterization of nanocrystalline calcium sulfate for use in osseous regeneration. Biomed Mater. Oct.2011 6:055007.
24. Dziak R, Barres Laura, Andreana Sebastiano. Recent patents on nanoceramics and bone regeneration and repair. Recent Patents in Regenerative Medicin. 2014; 94–102
25. Ionita CN, Hoffmann KR, Bednarek DR, Chityala R, Rudin S. Cone-beam micro-CT system based on LabVIEW software. J Digit Imaging. Sep.2008 21:296–305.
26. Rudin S, Wu Y, Kyprianou IS, Ionita CN, Wang Z, Ganguly A, Bednarek DR. Micro-angiographic detector with fluoroscopic capability. SPIE Medical Imaging. 2002
27. Patel V, Chityala RN, Hoffmann KR, Ionita CN, Bednarek DR, Rudin S. Self-calibration of a cone-beam micro-CT system. Medical Physics. 2009; 36:48.
28. Feldkamp LA, Davis LC, Kress JW. Practical cone-beam algorithm. Journal of the Optical Society of America. 1984; A1:612–619.
29. Bouxsein ML, Boyd SK, Christiansen BA, Guldberg RE, Jepsen KJ, Muller R. Guidelines for assessment of bone microstructure in rodents using micro-computed tomography. J Bone Miner Res. Jul.2010 25:1468–86.

30. Geraets WG, Verheij JG, van der Stelt PF, Horner K, Lindh C, Nicopoulou-Karayianni K, et al. Selecting regions of interest on intraoral radiographs for the prediction of bone mineral density. Dentomaxillofac Radiol. Oct.2008 37:375–9.

31. Guédon J, Autrusseau F, Amouriq Y, Bléry P, Bouler JM, Weiss P, Dallerit V. Exploring relationships between fractal dimension and trabecular bone characteristics. SPIE Medical Imaging. 2012

32. Liebovitch LS, Toth Tibor. A fast algorithm to determine fractal dimensions by box counting. physics Letters A. 1989; 141:386–390.

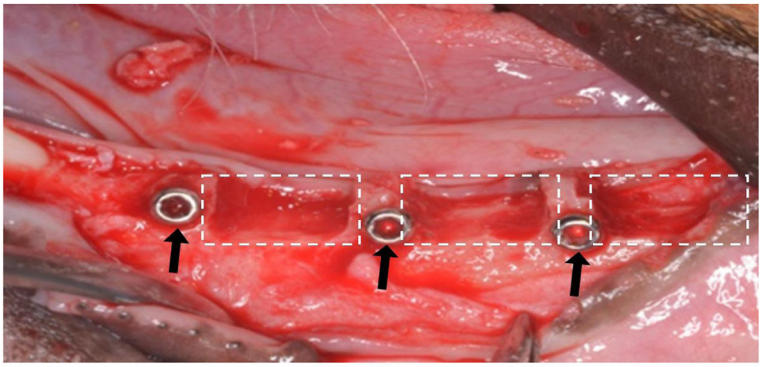

Figure 1.
Sample of a canine mandible just after making the defect. The dotted white boxes outline the defect location and the black arrows indicate the location of three metal screws used as markers.

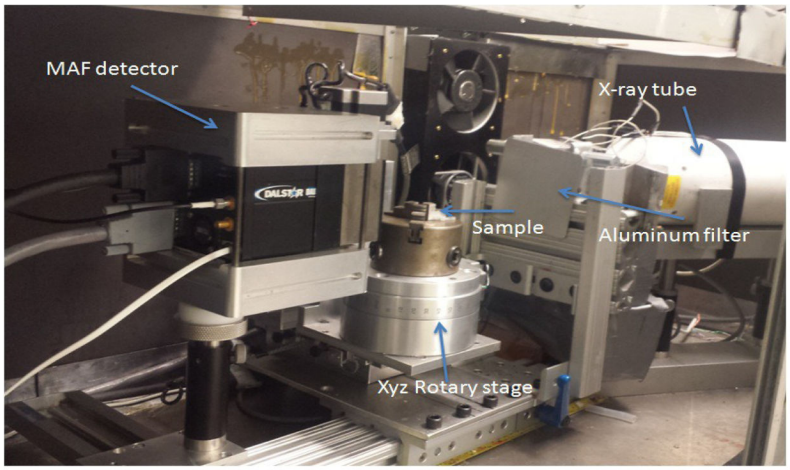

Figure 2.
The cone beam Micro-CT setup showing basic components of the system

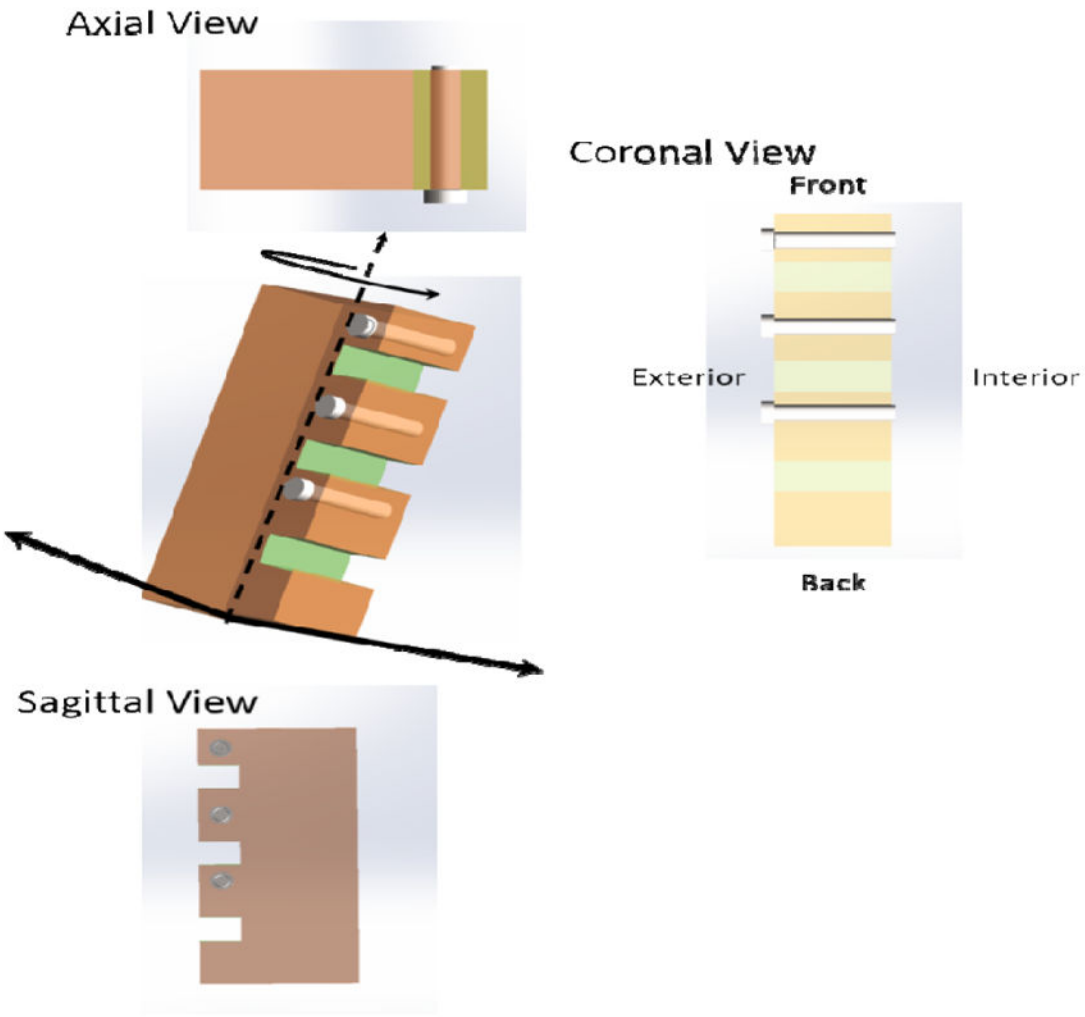

Figure 3.
Convention of multiplanar reformation and orientation of the marker with regard to the acquisition geometry.

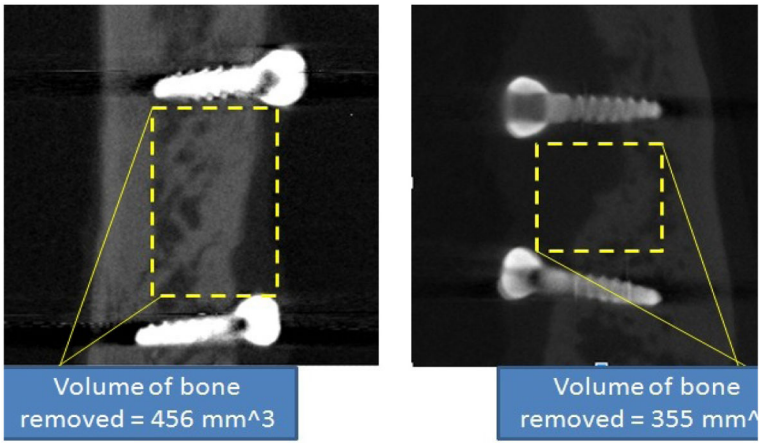

Figure 4.

Different volume of bone is removed because of asymmetry of object. Bone yield is per unit volume of bone in the given region of interest

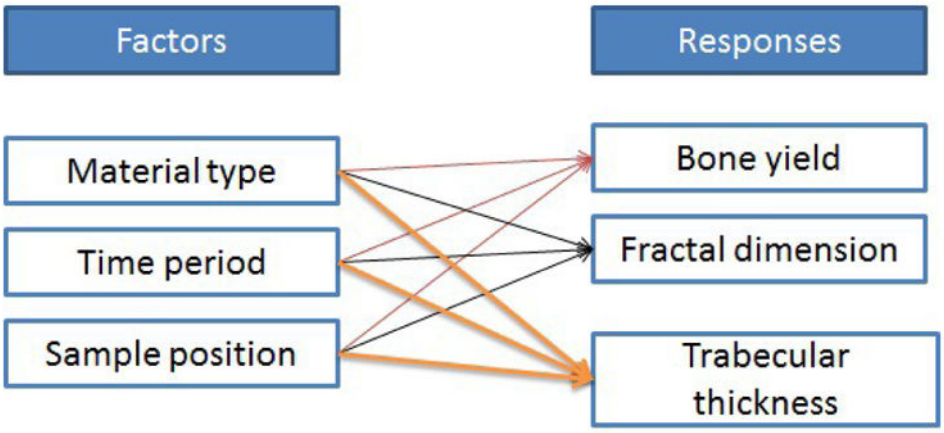

Figure 5.
Statistical experiment analysis design for ANOVA considering three factor and three responses

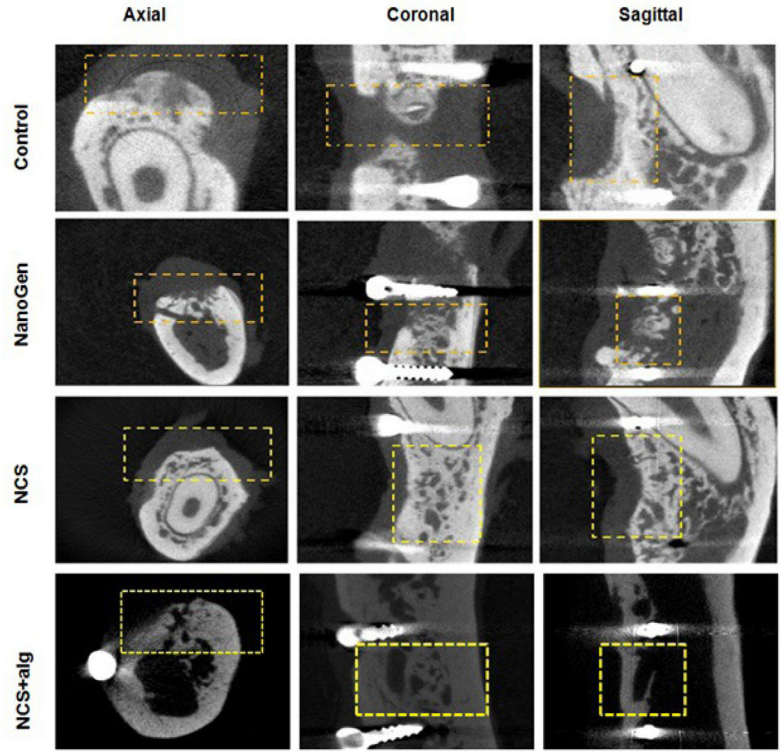

Figure 6.

First row shows different view of CT slices from control sample, an empty trough is clearly visible in marked square box in sagittal view. Second row shows samples treated with NanoGen material and significant growth is seen when compared with the control. Third and fourth row show samples treated with NCS and NCS+alg, proper trabecular structure and significantly more growth is seen when compared with the control and the sample treated with NanoGen

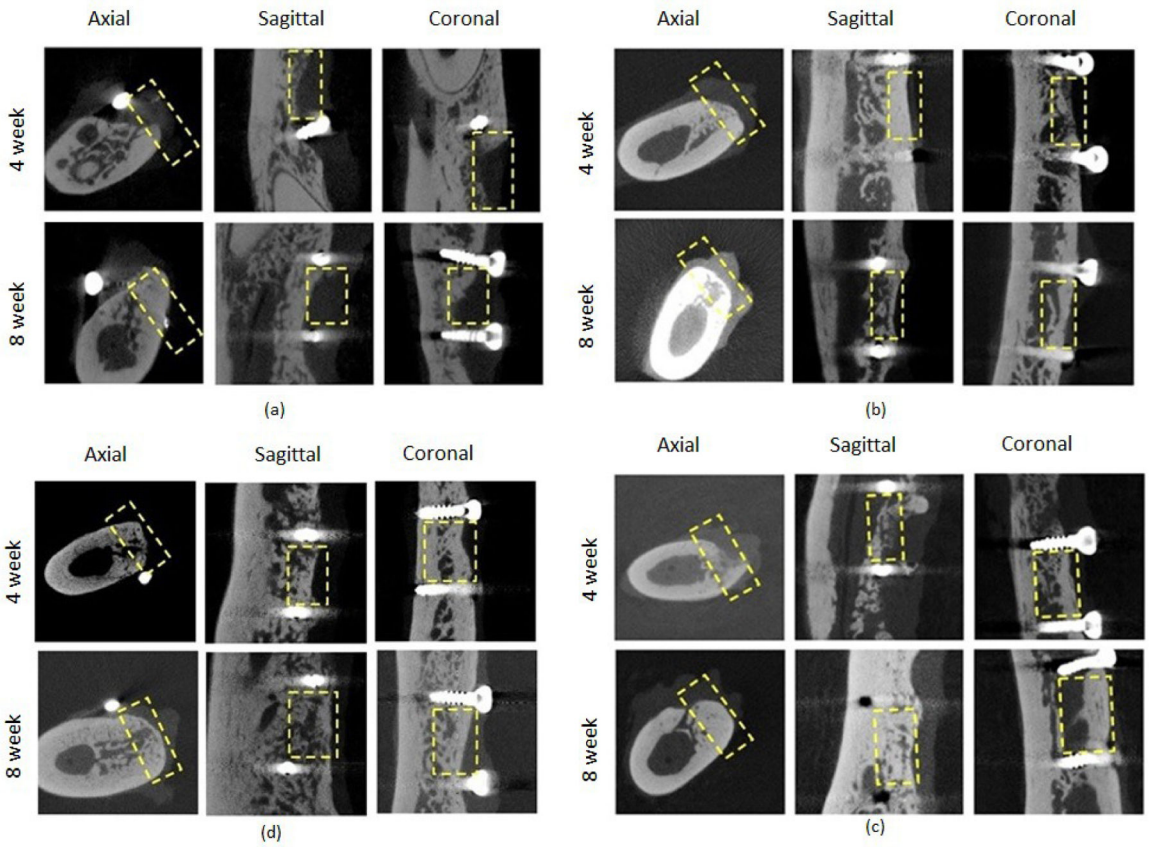

Figure 7.

Temporal comparison of control sample figure 7(a) and sample treated with NanoGen figure 7(b), sample treated with NCS figure 7(d) and sample treated using NCS+alginate figure 7(c). The region of interest in each sample is marked with the dotted line; perceptible differences are clearly observed in ROI boxes.

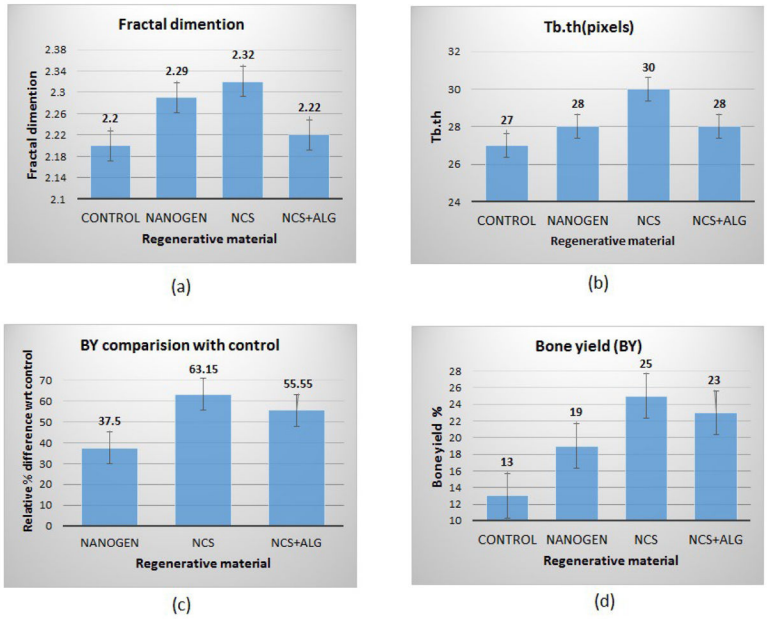

Figure 8.

The average values (4 and 8 Week) of imaging based parameters such as a) Fractal dimension b) Trabecular thickness and d) bone yield. Figure 8(c) shows the percentage difference in bone yield of regenerative material compared to the control sample.

Sensitivity Analysis

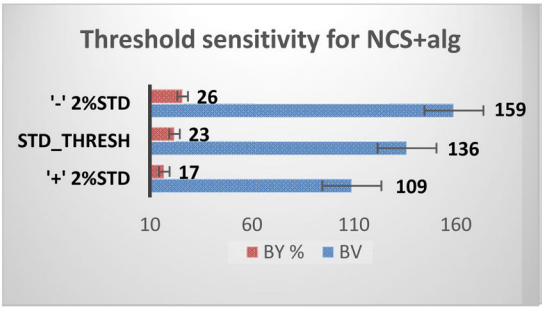

Figure 9(a)

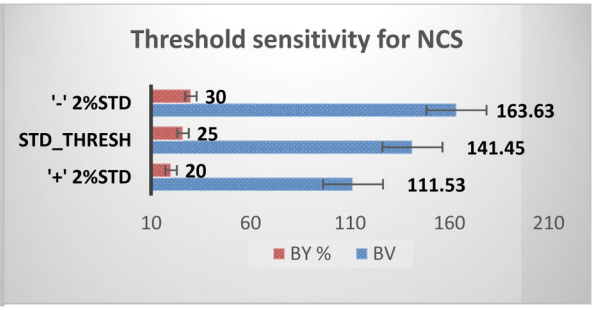

Figure 9(b)

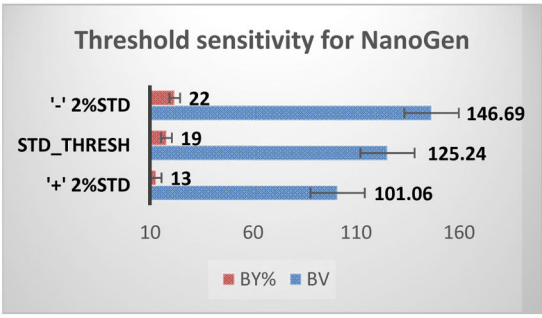

Figure 9(c)

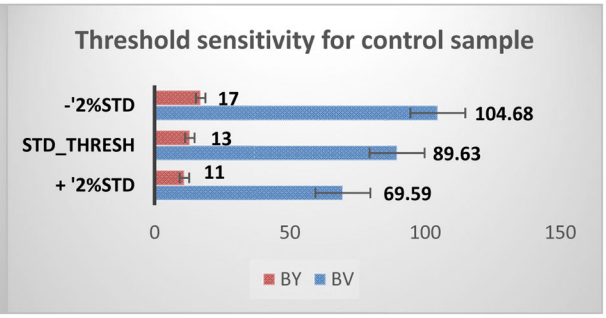

Figure 9(d)

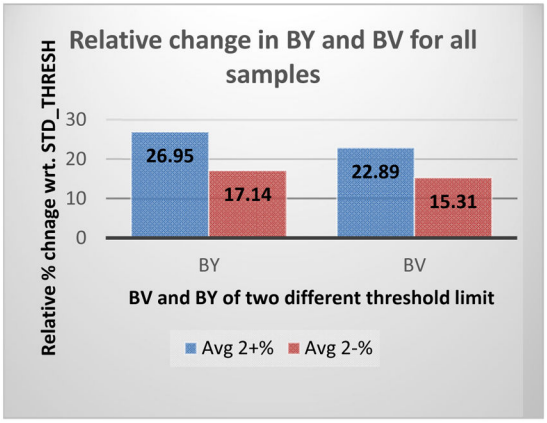

Figure 9(e)

Figure 9.

Sensitivity of segmentation and its effect on bone volume and bone yield calculation. Figure 9(a) (b) (c) and (d) shows threshold sensitivity of NCS+alg, NCS, NanoGen and Control samples for 8 and 4 week samples. Figure 9(e) Combined average sensitivity of thresholding for all samples and its effect on bone volume (BV) and bone yield (BY) calculation. (STD_THRESH – Threshold chosen by us, ±2% STD – Relative ±2% change in threshold with respect to our chosen value)